Human natural killer cells control *Plasmodium falciparum* infection by eliminating infected red blood cells

Qingfeng Chen[a,b], Anburaj Amaladoss[a], Weijian Ye[a,c], Min Liu[a], Sara Dummler[a], Fang Kong[a], Lan Hiong Wong[a], Hooi Linn Loo[a], Eva Loh[d], Shu Qi Tan[e], Thiam Chye Tan[e,f], Kenneth T. E. Chang[d,f], Ming Dao[a,g,1], Subra Suresh[h,i,1], Peter R. Preiser[a,c,1], and Jianzhu Chen[a,j,k,1]

[a]Interdisciplinary Research Group in Infectious Diseases, Singapore-MIT Alliance for Research and Technology, Singapore 138602; [b]Humanized Mouse Unit, Institute of Molecular and Cell Biology, Agency for Science, Technology and Research, Singapore 138673; [c]School of Biological Sciences, Nanyang Technological University of Singapore, Singapore 637551; Departments of [d]Pathology and Laboratory Medicine and [e]Obstetrics and Gynaecology, KK Women's and Children's Hospital, Singapore 229899; [f]Duke-National University of Singapore Graduate Medical School, Singapore 169857; Departments of [g]Materials Science and Engineering and [k]Biology and [j]Koch Institute for Integrative Cancer Research Massachusetts Institute of Technology, Cambridge, MA 02139; and Departments of [h]Materials Science and Engineering and [i]Biomedical Engineering, Carnegie Mellon University, Pittsburgh, PA 15213

Contributed by Subra Suresh, December 16, 2013 (sent for review October 25, 2013)

Immunodeficient mouse–human chimeras provide a powerful approach to study host-specific pathogens, such as *Plasmodium falciparum* that causes human malaria. Supplementation of immunodeficient mice with human RBCs supports infection by human *Plasmodium* parasites, but these mice lack the human immune system. By combining human RBC supplementation and humanized mice that are optimized for human immune cell reconstitution, we have developed RBC-supplemented, immune cell-optimized humanized (RICH) mice that support multiple cycles of *P. falciparum* infection. Depletion of human natural killer (NK) cells, but not macrophages, in RICH mice results in a significant increase in parasitemia. Further studies in vitro show that NK cells preferentially interact with infected RBCs (iRBCs), resulting in the activation of NK cells and the elimination of iRBCs in a contact-dependent manner. We show that the adhesion molecule lymphocyte-associated antigen 1 is required for NK cell interaction with and elimination of iRBCs. Development of RICH mice and validation of *P. falciparum* infection should facilitate the dissection of human immune responses to malaria parasite infection and the evaluation of therapeutics and vaccines.

malaria infection | humanized mouse model | LFA-1 | NK killing

Malaria is caused by infection with parasites of the *Plasmodium* species which are transmitted by bites of infected Anopheles mosquitoes. *Plasmodium* species are highly host specific. making it difficult to model human parasite infection in laboratory animals. So far, most in vivo experimental studies of malaria have been carried out with mouse and rat *Plasmodium* strains in rodents. Differences in invasion and disease pathology between human and rodent parasite species have impeded the translation of findings from rodents into human. The lack of appropriate small animal models also has hampered the evaluation of new drugs and vaccines before clinical trials (1).

To overcome this challenge, one approach is to supplement SCID mice with human RBCs. The resulting mice support a limited blood-stage *P. falciparum* infection (2–4). The need to inject large volumes of human RBCs repeatedly and to treat mice with anti-neutrophil antibody and highly toxic clodronate liposomes to suppress the rapid clearance of the injected human RBCs by macrophages in the recipient mice makes working with this system difficult. More recently NOD-SCID Il2rg$^{-/-}$ (NSG) mice have been shown to support a more efficient *P. falciparum* infection without the treatment of clodronate liposomes or anti-neutrophil antibody (5). Furthermore, a recent report shows the development of liver-stage *P. falciparum* infection in immunocompromised and fumarylacetoacetate hydrolase-deficient (*Fah*$^{-/-}$, *Rag2*$^{-/-}$, *Il2rg*$^{-/-}$) (FRG) mice. Backcrossing of FRG mice to the NOD background and supplementing the resulting mice with human RBCs led to reproducible transition from liver-stage infection to blood-stage infection (6). Despite such progress, none of the existing mouse models of human parasite infection has a human immune system.

The immune system plays a critical role in the control of parasite infection. Studies in mice using mouse *Plasmodium* strains have shown that mouse immune cells such as natural killer (NK) cells, T cells, dendritic cells, and B cells all contribute to anti-parasitic immunity (7–10). Notably, depletion of NK cells in a mouse model of *Plasmodium chabaudi* infection results in more severe disease associated with higher parasitemia and mortality (11). In vitro, *P. falciparum*-infected human RBCs are shown to interact with human NK cells, leading to the induction of IFN-γ (12). Compared with *P. falciparum* schizonts, live infected RBCs (iRBCs) induce more rapid activation and more production of IFN-γ by NK cells (13). More recently, it has been shown that, in addition to IFN-γ, activated human NK cells also produce perforin and granzyme against *P. falciparum*-infected RBCs (14). However, because of the lack of appropriate models, little is known about the role of human NK cells in the control of *P. falciparum* infection in vivo. NK cells are cytolytic and can lyse virus-infected cells and tumor cells (15). However, whether

Significance

Study of human immune responses to malaria parasite infection has been hampered by a lack of small animal models. Although immunodeficient mice supplemented with human RBCs support human parasite infection, these animals lack a human immune system. We have overcome this obstacle by developing mice that possess both human RBCs and immune system and that support multiple cycles of *Plasmodium falciparum* infection. We further show that human natural killer cells preferentially interact with and kill infected RBCs in a contact-dependent manner. The small animal model reported here likely will facilitate the dissection of human immune responses to malaria parasite infection and the evaluation of therapeutics and vaccines.

Author contributions: Q.C., M.D., S.S., P.R.P., and J.C. designed research; Q.C., A.A., W.Y., M.L., F.K., L.H.W., and H.L.L. performed research; A.A., S.D., E.L., S.Q.T., T.C.T., K.T.E.C., and M.D. contributed new reagents/analytic tools; Q.C., W.Y., M.L., M.D., S.S., P.R.P., and J.C. analyzed data; and Q.C., S.S., P.R.P., and J.C. wrote the paper.

The authors declare no conflict of interest.

Freely available online through the PNAS open access option.

[1]To whom correspondence may be addressed. E-mail: mingdao@mit.edu, suresh@cmu.edu, prpreiser@ntu.edu.sg, or jchen@mit.edu.

This article contains supporting information online at www.pnas.org/lookup/suppl/doi:10.1073/pnas.1323318111/-/DCSupplemental.

NK cells also can eliminate parasite-infected RBCs directly has not been demonstrated comprehensively.

In our study of humanized mice, we previously had developed a simple and effective method of enhancing human cell reconstitution by hydrodynamic expression of human cytokines. Expression of human IL-15 and Flt-3/Flk-2 ligand (Flt-3L) enhances the reconstitution of human NK cells, monocytes, and macrophages (16). In this study, we have constructed humanized mice that have an optimized human immune cell reconstitution as well as high levels of human RBCs through supplementation. We show that such humanized mice support an efficient infection by *P. falciparum.* Depletion of human NK cells, but not macrophages, in these mice results in a significant increase in parasitemia. Our additional studies in vitro show that NK cells interact preferentially with iRBCs and become activated, resulting in the elimination of iRBCs in a contact-dependent manner. We further show that the cell adhesion molecules lymphocyte-associated antigen 1 (LFA-1) and to some extent DNAX accessory molecule 1 (DNAM-1) mediate NK cell interaction with and elimination of iRBCs. Development of humanized mice with robust reconstitution of human immune cells and human RBCs and validation of the model for *P. falciparum* infection should facilitate the dissection of human immune responses to malaria parasite infection and the evaluation of therapeutics and vaccines.

Results

RBC-Supplemented, Immune Cell-Optimized Humanized Mice Support Robust *P. falciparum* Infection. To construct humanized mice that have an optimized human immune cell reconstitution as well as high levels of human RBCs, we expressed human IL-15 and Flt-3L in humanized mice to enhance the reconstitution of human NK cells, monocytes, and macrophages (16) and supplemented the cytokine-treated mice with human RBCs. Specifically, humanized mice with 40% or more human leukocyte reconstitution in peripheral blood mononuclear cells (PBMCs) were injected with plasmids encoding human IL-15 and Flt3L. One day after plasmid injection, mice were given a daily injection of 1 mL of human RBCs. After supplementing RBC for 7 d, mice were bled and analyzed for human RBC and human immune cell reconstitution by flow cytometry. A significant fraction (25.1 ± 9.8%, $n = 10$) of RBCs stained positive for human CD235ab (Fig. 1*A*), and a large fraction (42.1 ± 11.7%, $n = 10$) of PBMCs stained positive for human CD45 (Fig. 1*B*). Among various human immune cell types, significant levels of $CD56^+$ NK cells (14.2 ± 3.6%), $CD14^+$ monocytes/macrophages (4.5 ± 1.3%), $CD3^+$ T cells (33.2 ± 12.2%), and $CD19^+$ B cells (51.6 ± 15.4%) were present (Fig. 1*C*). Among NK cells, both $CD56^{bright}CD16^-$ and $CD56^{dim}CD16^+$ populations were detected, and very few cells were positive for CD69 (Fig. S1). However, NK cells were activated by IL-15 in vitro, suggesting that NK cells in the blood of cytokine-treated mice were not activated. These results show that RBC supplementation into cytokine-treated humanized mice leads to high levels of both human RBC and immune cell reconstitution. We refer to these RBC-supplemented, immune cell-optimized humanized mice as "RICH" mice.

To determine the efficiency of parasite infection, RICH mice were injected i.v. with 5×10^6 synchronized ring-stage parasites from the 3D7 strain of *P. falciparum* 7 d after RBC supplementation. The infected mice were given human RBC supplementation daily throughout the experiment. Blood samples were taken every 48 h to measure parasitemia by microscopy. At all time points, significant levels of iRBCs were detected, with the majority of the parasites being at the ring stage. Over a 240-h period, blood parasitemia increased steadily from 0.01 ± 0.001% at 48 h to 0.13 ± 0.02% at 240 h (Fig. 1*D*; $n = 10$). (The parasitemia level would be four times the whole-blood value when normalized to human RBC frequency in the whole blood). These results show that RICH mice can support a significant level of *P. falciparum* infection in the presence of an optimized human immune system and provide an in vivo system for evaluating the role of specific human immune cell types in controlling parasite infection.

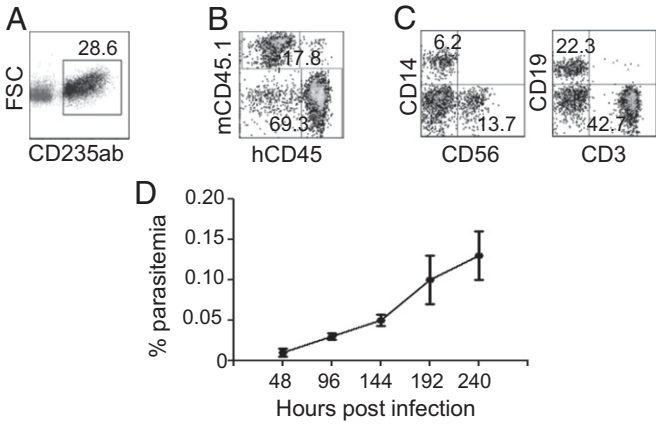

Fig. 1. RICH mice support a robust *P. falciparum* infection. Humanized mice were injected hydrodynamically with plasmids encoding human IL-15 (50 μg) and Flt3L (10 μg) on day zero. Beginning 1 d after plasmid injection, mice were injected i.p. daily with 1 mL human RBCs. After 7 d of RBC supplementation, mice were infected i.v. with 5×10^6 ring-stage 3D7 parasites and given daily RBC supplementation throughout the experiment ($n = 10$). (*A*–*C*) Human RBC and immune cell reconstitution before parasite infection (7 d after plasmid injection). Shown are representative CD235ab vs. forward scatter (FSC) profiles of whole blood (*A*), human CD45 (hCD45) vs. mouse CD45.1 (mCD45) staining profiles of PBMCs (*B*), and human CD56 vs. CD14 and CD3 vs. CD19 staining profiles gating on human $CD45^+$ cells (*C*). The numbers indicate the percentage of cells in the gated regions. The mean ± SEM ($n = 10$) are shown in *Results*. (*D*) Quantification of parasitemia in RICH mice at different time points. Data are shown as percentage (mean ± SEM) of iRBCs among total RBCs and are a compilation from two independent experiments with five mice in each experiment.

NK Cells Play a Critical Role in Controlling Parasite Infection. We next investigated whether human immune cells respond to *P. falciparum* infection in RICH mice. To determine the role of human NK cells and macrophages, RICH mice were injected with anti-human CD56 and anti-human CD14 antibody to deplete NK cells and macrophages, respectively. As shown in Fig. 2*A*, the percentages of $CD56^+$ NK cells (13.5 ± 2.1%, $n = 6$) and $CD14^+$ monocytes/macrophages (4.3 ± 1.1%, $n = 6$) in PBMCs of RICH mice were not affected significantly by PBS injection. Twenty-four hours after a single injection of anti-human CD56 (clone HCD56), the level of NK cells was reduced by ~25-fold to ~0.4%, as revealed by staining with an anti-CD56 antibody (clone MEM188) that recognizes a different epitope on CD56. This result was confirmed further by staining for the NK cell marker NKp46 (Fig. S2). Similarly, anti-human CD14 (clone M5E2) treatment reduced the level of monocytes/macrophages by ~40-fold to ~0.1%, as revealed by staining with an anti-CD14 antibody (clone HCD14) that recognizes a different epitope on CD14. This result was confirmed further by staining for CD11b and HLA-DR (Fig. S2). The depletion was sustained for at least 3 d. These mice were infected i.v. with 5×10^6 purified 3D7 ring-stage parasites 24 h after antibody treatment. Two days later, the level of parasitemia in the blood was quantified by microscopy. In the PBS-treated mice, parasitemia was 0.01 ± 0.002% ($n = 6$), the same as in untreated RICH mice (compare Figs. 2*B* and 1*D*). In contrast, parasitemia increased about sevenfold to 0.074 ± 0.02% ($n = 6$) in NK cell-depleted mice. Depletion of human monocytes/macrophages did not lead to any significant change in parasitemia. These results show that human NK cells, but not macrophages, play a significant role in the immediate control of *P. falciparum* infection in RICH mice.

We measured the level of human IFN-γ and IL-6 in the sera of infected mice 2 d after infection. In PBS-treated RICH mice, the levels of IFN-γ and IL-6 were 189.1 ± 20.2 pg/mL and 130.2 ± 13.6 pg/mL ($n = 6$), respectively (Fig. 2 *C* and *D*). In NK cell-depleted RICH mice, the levels of IFN-γ and IL-6 were reduced

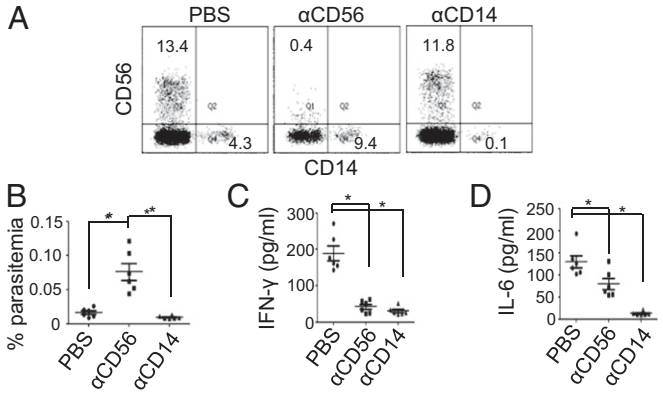

Fig. 2. NK cells play a critical role in the control of parasite infection. Seven days after cytokine treatment and 6 d after RBC supplementation, RICH mice were injected with PBS, anti-human CD56 antibody (αCD56), or anti-human CD14 antibody (αCD14). One day later, mice were bled, and the levels of human NK cells and monocytes/macrophages in PBMCs were analyzed by flow cytometry. Then mice were infected immediately with 5×10^6 3D7 ring-stage parasites. Two days later, parasitemia was analyzed in the whole blood by microscopy, and human IFN-γ and IL-6 in the serum were measured by ELISA. (*A*) Depletion of human $CD56^+$ NK cells and $CD14^+$ monocytes/macrophages in treated mice. Shown are representative CD14 vs. CD56 staining profiles of $hCD45^+$ PBMCs of control, αCD56-, and αCD14-treated mice. The numbers indicate the percentage of cells in the gated regions. (*B–D*) Comparison of parasitemia (*B*) and serum levels of human IFN-γ (*C*) and IL-6 (*D*) in the three groups of mice. Each symbol represents one mouse. Data represent mean ± SEM. $*P < 0.01$. $n = 6$ for each group.

to 42.4 ± 7.0 pg/mL and 79.8 ± 12.3 pg/mL ($n = 6$), respectively. Depletion of macrophages resulted in even a more dramatic reduction of both IFN-γ (23.8 ± 4.6 pg/mL) and IL-6 (9.3 ± 0.2 pg/mL). Because depletion of macrophages did not affect parasitemia significantly, these cytokines probably are not involved in the effect of NK cells on parasite infection.

Human NK Cells Respond to and Eliminate iRBCs in Vitro. To investigate how human NK cells control parasite infection, we established an in vitro culture system using purified NK cells, RBCs, and parasites. Human NK cells were purified from adult PBMCs and cultured with human RBCs and 3D7 schizonts at a ratio of 10:250:1. Video microscopy revealed that NK cells migrated and interacted with RBCs randomly. However, when NK cells encountered iRBCs, they formed stable contacts as soon as 2 h after incubation (Fig. S3). Quantification showed that, on average, NK cell contact was 11-fold longer with iRBCs than with uninfected RBCs (4,075 ± 617 s vs. 359 ± 62 s) (Fig. 3*A*), indicating preferential interaction between NK cells and iRBCs. Correspondingly, NK cells were activated to express CD69 in cultures in the presence of parasites as early as 4 h but were not activated to express CD69 in cultures in the absence of parasites (Fig. 3*B*). The fraction of NK cells that were induced to express CD69 reached ∼24% after 24 h of culture, suggesting that NK cells are activated by iRBCs in vitro. Further analysis revealed that, although the levels of NKp46, CD2, CD8, NKG2D, and NKG2a tended to be slightly higher on $CD56^+$ $CD69^+$ cells than on $CD56^+CD69^-$ NK cells, the difference was not significant.

We quantified parasitemia in the culture at 48 and 96 h by microscopy. The difference in parasitemia in cultures with (1.9 ± 0.2%) and without (0.9 ± 0.1%) NK cells already was significant (∼twofold) at 48 h, and this difference became even more dramatic (6.0 ± 0.2% vs. 1.6 ± 0.1%, ∼3.5-fold) at 96 h. These results were confirmed further by flow cytometry. Cultured cells were stained with the DNA-staining dye Hoechst and CD56 at 48 and 96 h. The iRBCs were positive for Hoechst but negative for CD56, but NK cells were positive for both (Fig. 3*C*). After culture for 48 h, 1.8 ± 0.1% of RBCs stained positive for Hoechst in the absence of NK cells, indicating infection by parasites. In the presence of NK cells, the percentage was reduced to 0.8 ± 0.1% (twofold). This reduction was more dramatic at 96 h (6.1 ± 0.2% vs. 1.6 ± 0.1%, ∼3.8-fold), as was consistent with data from microscopy. Human NK cells purified from humanized mice also exhibited similar antiparasite effects in culture (Fig. 3*D*).

To gain direct evidence of NK cell killing of iRBCs, we visualized NK cell–iRBCs coculture by video microscopy. After 12 h of culture, iRBCs that formed stable contact with NK cells became flattened, indicating leakage of cell content and loss of cell volume, whereas iRBCs without NK cell contact did not (Fig. S4). Furthermore, we tested whether inhibition of perforin activity by concanamycin A (CMA) interferes with elimination of iRBCs by NK cells. As shown in Fig. 3*E*, in the absence of NK cells, the percentage of iRBCs was ∼8%. As expected, this percentage was reduced (to ∼4%) in the presence of NK cells. The percentage was elevated (to ∼7%) when CMA was added into

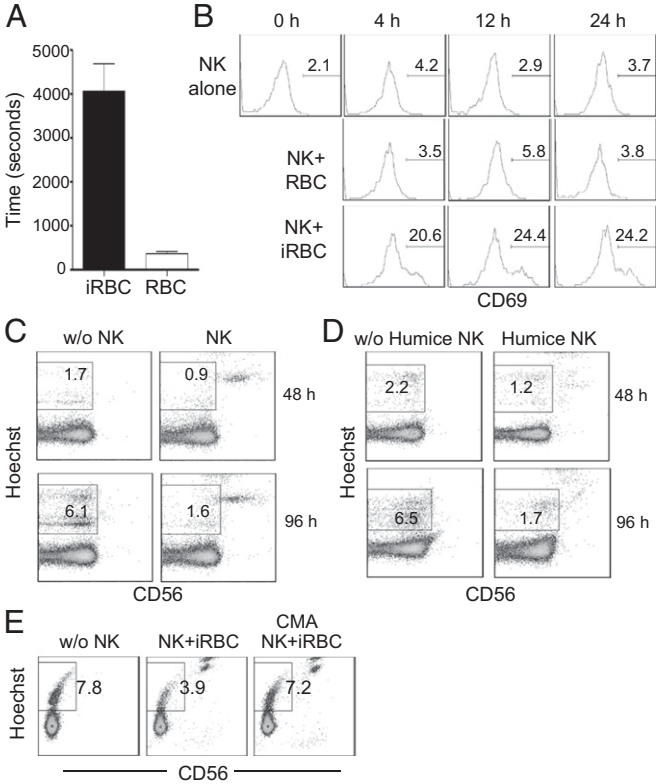

Fig. 3. Human NK cells respond to and eliminate iRBCs in vitro. Human RBCs were incubated with purified 3D7 schizonts in the presence or absence of purified human NK cells. Some cultures were visualized by video microscopy to follow NK cell migration and interaction with RBCs. Some cultures were stained for CD69 to monitor NK cell activation or were stained by Hoechst plus anti-CD56 to quantify parasitemia. (*A*) Comparison of the lengths of time during which NK cells interact with infected vs. uninfected RBCs. The data are averages of 100 NK cells interacting with infected or uninfected RBCs. (*B*) Comparison of CD69 expression by $CD56^+$ NK cells at the indicated time points of culture. The numbers indicate the percentages of $CD69^+$ cells. (*C*) Representative CD56- vs. Hoechst-staining profiles of cultured cells at 48 and 96 h. (*D*) Humanized mice were hydrodynamically injected with plasmids encoding human IL-15 and Flt3L to enhance reconstitution of human NK cells. Seven days later, NK cells were purified from blood, spleen, lung, and liver and were used in the culture as above. Shown are CD56- vs. Hoechst-staining profiles of cultures with or without NK cells at 48 and 96 h. (*E*) NK cells were cultured with RBCs and 3D7 schizonts in the presence or absence of CMA. Parasitemia was measured by flow cytometry 96 h after coculture. Representative CD56- vs. Hoechst-staining profiles of cultured cells are shown. The numbers in *B*– *E* indicate the percentages of iRBCs among total RBCs.

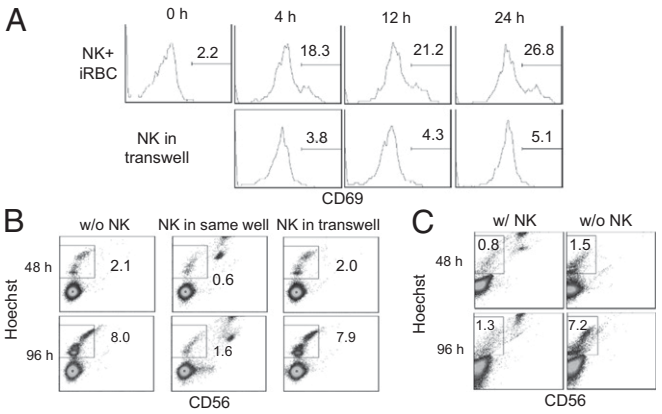

Fig. 4. Cell–cell contact is required for NK cell activation and killing of iRBCs. (*A* and *B*) Human RBCs were infected with purified 3D7 schizonts in the absence or presence of human NK cells in the same well or in a separate compartment in the transwell. NK cells were assayed for CD69 expression at 4, 12, and 24 h, and parasitemia was measured at 96 h by flow cytometry. (*A*) Comparison of CD69 expression by $CD56^+$ NK cells in the same well or in a separate compartment in the transwell at the indicated time points of culture. The numbers indicate percentages of $CD69^+$ cells. (*B*) Representative CD56- vs. Hoechs- staining profiles of cultured cells at 96 h. (*C*) Transwell assay of the killing of iRBCs by NK cells. NK cells were cultured with RBCs and 3D7 schizonts in one chamber (w/ NK). The other chamber contained only RBCs and parasites (w/o NK). Parasitemia in both chambers was quantified by flow cytometry at 48 and 96 h. Shown are representative CD56- vs. Hoechst-staining profiles of cells from the two chambers. The numbers in *B* and *C* indicate the percentage of iRBCs among total RBCs.

the coculture, suggesting that CMA blocked the elimination of iRBCs by NK cells. Together, these results show that NK cells from human and humanized mice can respond to and kill iRBCs in vitro.

Cell–Cell Contact Is Required for NK Cell Activation and Killing of iRBCs. We further determined the requirement for cell–cell contact and soluble factors in NK cell activation and killing of iRBCs. NK cells purified from human PBMCs were cultured with human RBCs and purified 3D7 schizonts in the same well or in different compartments of the transwell. The induction of CD69 on NK cells was assayed by flow cytometry 24 and 48 h later. As shown in Fig. 4*A*, a significant fraction of NK cells was induced to express CD69 as early as 4 h after culture in the same well (~18%), and the fraction of $CD69^+$ NK cells increased to ~27% by 24 h. In contrast, very few NK cells cultured in separate compartments of the transwell expressed CD69. Consistently, after culture for 96 h, parasitemia was reduced from ~8.0% in the absence of NK cells to ~1.6% when NK cells were present in the same well, whereas parasitemia was not significantly reduced when NK cells were cultured in separate compartments of the transwell (Fig. 4*B*).

To test further whether cell–cell contact is required for NK cell killing of iRBCs, we performed transwell cultures in which one chamber contained NK cells, RBCs, and parasites and the other chamber contained only RBCs and parasites. Parasitemia in both chambers was quantified by flow cytometry after culture for 48 and 96 h. By 96 h in culture, parasitemia was ~1.3% in the chamber containing NK cells but was ~7.2% in the chamber without NK cells (Fig. 4*C*). Thus, both the activation of NK cells and NK cell killing of iRBCs require the direct contact of NK cells with iRBCs.

LFA-1 Is Involved in NK Cell Interaction with and Killing of iRBCs. To identify cell-surface receptors that might be involved in NK cell interaction with and killing of iRBCs, we tested an extensive panel of cell-surface receptors, including NKG2D, NKp30, NKp44, NKp46, and 2B4, which are known to be involved in NK cell killing of tumor cells and virus-infected cells, and CD2, DNAM-1, and LFA-1, which mediate cell–cell adhesion (17). Purified human NK cells were cultured with human RBCs and 3D7 schizonts in the absence or presence of blocking antibodies, and the percentages of iRBCs were quantified 96 h later. As shown in Fig. 5*A*, the percentage of iRBCs was ~6% without the addition of NK cells into the culture; this percentage was reduced to ~2% with the addition of NK cells. The percentages remained at ~2% when antibodies were added to block NKG2D, NKp30, NKp44, NKp46, 2B4, and CD2 individually, indicating that these molecules are not involved in the killing of iRBCs by NK cells. In contrast, the percentages of iRBCs were ~6% and 4%, respectively, when LFA-1 and DNAM-1 were blocked, suggesting a complete or partial blocking of iRBC killing by NK cells.

To gain insight into how LFA-1 is involved in the elimination of iRBCs by NK cells, we investigated the effect of an LFA-1–blocking antibody on the interaction of NK cells with iRBCs and the activation of NK cells. The length of time that NK cells interacted with iRBCs was reduced from an average of 4,236 ± 718 s in the absence of the LFA-1–blocking antibody to 428 ± 109 s in the presence of the blocking antibody (Fig. 5*B*). The latter time was virtually the same as the length of time that NK cells interacted with noninfected RBCs (Fig. 3*A*). Furthermore, in the presence of the LFA-1–blocking antibody, only 13% of NK cells expressed CD69 (Fig. 5*C*), a fourfold reduction compared with the expression of CD69 in the absence of the LFA-1–blocking antibody (52%). These results suggest that LFA-1 mediates the elimination of iRBCs by NK cells by promoting the interaction NK cell with iRBCs and the activation of NK cells.

Discussion

By supplementing immunodeficient mice with human RBCs, recent studies (2–6) have established various mouse models that support infection by human *Plasmodium* parasites. However,

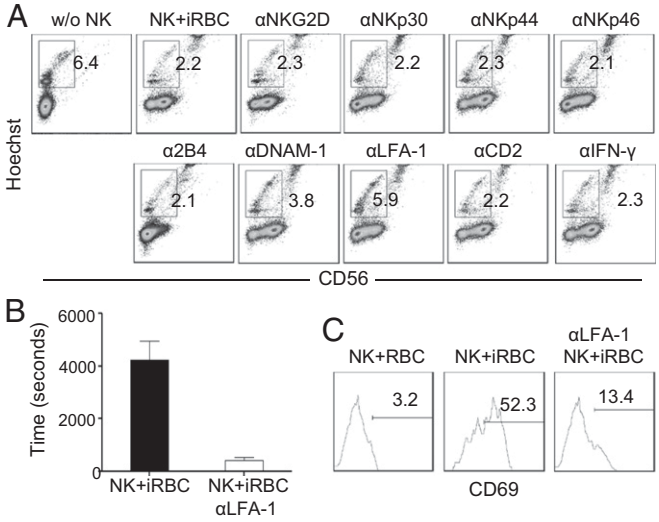

Fig. 5. LFA-1 is involved in NK cell interaction with and killing of iRBCs. (*A*) NK cells were cultured with RBCs and 3D7 schizonts in the presence or absence of the indicated blocking antibodies, and parasitemia was quantified by flow cytometry 96 h later. Shown are representative CD56- vs. Hoechst-staining profiles of cells. The numbers indicate the percentage of iRBCs among total RBCs. (*B* and *C*) NK cells were cultured with RBCs and 3D7 schizonts in the presence or absence of the LFA-1–blocking antibody. (*B*) The culture was visualized by video microscopy. Shown are the lengths of time NK cells interact with iRBCs with (αLFA-1) and without (NK+iRBCs) the blocking antibody. The data shown are the average of 20 NK cells that interacted with iRBCs. (*C*) NK cells were assayed for CD69 expression at 48 h. Shown is CD69 expression by $CD56^+$ NK cells in the presence or absence of the LFA-1–blocking antibody. The numbers indicate percentages of $CD69^+$ cells.

a common deficiency of these models is the lack of a human immune system. A mouse model that has a human immune system and that supports infection by human *Plasmodium* parasites is highly desirable, because it would facilitate both dissection of human immune responses to parasite infection and the evaluation of the efficacy of vaccines and therapeutics that require the presence of a human immune system. Toward this goal, we supplemented humanized mice that are optimized for human immune cell reconstitution with human RBCs. Humanized mice were injected with IL-15– and Flt3L-expressing plasmids to enhance human immune cell reconstitution and then were supplemented daily with human RBCs. One week after cytokine expression and RBC supplementation, human immune cell reconstitution reached the peak level, and the percentage of human RBCs reached ~25%. When these RICH mice were infected with the 3D7 strain of *P. falciparum,* parasitemia increased steadily over time from 0.01% at 48 h postinfection to 0.13% at 240 h postinfection. In NSG mice with human RBC supplementation, parasitemia can reach as high as 14% at 240 h postinfection (5). In RICH mice, the parasitemia is 100-fold lower (~0.13%) at the same point in time but is closer to the levels found in most malaria patients (18). The difference between RBC-supplemented NSG mice and RICH mice is the presence of a human immune system in the latter mice, so the differences in parasitemia in the two mice models suggests that the human immune system has an important role in controlling parasite infection in RICH mice (see below). Because RBCs do not express major histocompatibility complex molecules (19), the supplemented human RBCs and the reconstituted human immune cells in humanized mice can be from different donors, thus making it easier to construct RICH mice for *Plasmodium* infection.

Establishment of the RICH mouse model that supports robust parasite infection in the presence of the human immune system enabled us to investigate the role of human NK cells and macrophages in the control of parasite infection. Depletion of human NK cells, but not macrophages, resulted in a sevenfold increase in blood parasitemia at 48 h postinfection. Because humanized mice have only human and no mouse NK cells, this result suggests that human NK cells play a critical role in the immediate control of parasite infection. In humanized mice, both human and mouse macrophages are present. The lack of any significant effect following depletion of human macrophages could mean that human macrophages are not required for controlling the parasite load at an early stage of infection or that the effect of human macrophage depletion is masked by the presence of mouse macrophages. It is notable that depletion of either human NK cells or macrophages resulted in similar reductions of human IFN-γ and IL-6 in the sera, suggesting that these cytokines do not mediate the antiparasite effect of NK cells. This interpretation was supported further by in vitro studies showing that NK cells exert their function through direct contact with iRBCs and that neutralization of IFN-γ does not diminish the NK cell effect (Fig. 5). Studies suggest that IFN-γ is produced by NK cells in malaria patients (20) and during in vitro culture with iRBCs (13). However, the role of IFN-γ in the antimalaria response is poorly understood. Our results exclude a significant direct antimalaria effect of IFN-γ or any autocrine effect on NK cells. It remains possible, however, that IFN-γ may be important for the downstream activation of human adaptive immune responses. The RICH mice described here provide an in vivo platform for evaluating human adaptive responses, especially T cells, against malaria parasites.

We elucidated how NK cells control parasite infection by further in vitro studies. Although human NK cells from PBMCs have been shown to respond to iRBCs by producing the proinflammatory cytokines IFN-γ, IL-12, and IL-18 as well as the cytotoxic molecules perforin and granzyme (12–14, 21, 22), most previous in vitro studies relied on culturing iRBCs with total PBMCs, which are a mixture of various immune cell populations. In our study, we used purified human NK cells from PBMCs to obtain direct evidence that human NK cells are able to migrate, bind, and eliminate iRBCs in the absence of other immune cell types. We show that, although NK cells appear to scan RBCs randomly in the culture, upon encounter they interact with iRBCs much longer than with uninfected RBCs. The prolonged interaction leads to the activation of NK cells, as indicated by expression of CD69. Once NK cells are activated, they eliminate iRBCs in a contact-dependent manner. By video microscopy, we observed flattening of iRBCs after interaction with NK cells but did not observe any sign of phagocytosis of iRBCs by NK cells. The flattening of iRBCs likely results from the leakage of cell content and loss of cell volume—and hence the killing—of iRBCs. Supporting this interpretation, the inhibition of perforin by CMA significantly reduces the elimination of iRBCs, a result that is consistent with previous observations that perforin and granzymes are induced when NK cells interact with iRBCs (14). Although data from previous research and our present study suggest that NK cells inhibit malaria parasite infection by killing the iRBCs, it remains possible that other mechanisms also may be involved. Although further studies are required to elucidate the detailed mechanisms, our present findings show that both the activation of NK cells by iRBCs and then the elimination of iRBCs by NK cells are contact dependent.

We further evaluated the classical NK cell activation and adhesion receptors in interaction with and elimination of iRBCs. Blocking NKG2D, NKp30, NKp44, NKp46, CD2, DNAM-1, and 2B4 did not diminish the killing of iRBCs by NK cells, suggesting that these receptors are not involved in the recognition or killing of iRBCs by NK cells. We found that anti–LFA-1 completely and anti–DNAM-1 partially inhibited the killing of iRBCs by NK cells. These results are consistent with the observation that DNAM-1 is physically and functionally associated with LFA-1 (23). The observed difference between blocking LFA-1 and DNAM-1 suggests that LFA-1 plays a more dominant role. Besides its function in cell adhesion, LFA-1 also is known to contribute to NK cell cytotoxicity (24). We found that blocking of LFA-1 almost completely abolished the preferential interaction of NK cells with iRBCs and significantly blocked the activation of NK cells, suggesting that LFA-1 is required for the interaction between NK cells and iRBCs. The known ligand of LFA-1 is ICAM-4, which is expressed by RBCs (25). Because NK cells preferentially interact with iRBCs rather than with uninfected RBCs, NK cells may recognize other molecules, including parasite proteins, on iRBCs. Elucidation of the molecular nature of these interactions is critical to understand the underlying mechanism of the NK cell response to *P. falciparum*-infected RBCs.

By supporting a robust parasite infection in the presence of human immune system, RICH mice likely will find wide application in dissecting human immune responses to parasite infection in a physiological setting. It has been demonstrated that a human immune system and hepatocytes can be reconstituted in the same humanized mice (26). Similarly, we have shown previously that engraftment of $CD34^+$ cells from fetal liver into NSG mice leads to reconstitution of human immune cells as well as human hepatocytes in the mouse liver (27). By supplementing human RBCs in such humanized mice, it may be possible to extend this model for both the blood and liver stage of *Plasmodium* infection in the presence of a human immune system.

Materials and Methods

Mice. NSG mice were purchased from the Jackson Laboratories and maintained under specific pathogen-free conditions in the animal facilities at National University of Singapore (NUS). Humanized mice were constructed as follows: Newborn pups (within 48 h of birth) were irradiated with 100 cGy using a gamma radiation source and were injected intracardially with $CD34^+$ cells from fetal liver (2×10^5 cells per recipient). Mice were analyzed for human leukocyte reconstitution at age 10–12 wk by staining for human CD45 and mouse CD45 (16). To make RICH mice, mice with 40% or more human leukocyte reconstitution in the PBMCs were injected hydrodynamically with plasmids encoding human IL-15 and Flt3L. Beginning 1 d after plasmid injection, mice were i.p. injected daily with human RBC [resuspended in RPMI medium containing 50% (vol/vol) heat-inactivated human serum (Invitrogen)].

Seven days later, the levels of human RBCs in humanized mice were quantified by staining peripheral blood cells with anti-human CD235ab antibody (BioLegend). Mice with a minimum of 20% human RBC reconstitution were used for subsequent experimentation. To deplete human NK cells and macrophages, anti-human CD56 (clone HCD56; BioLegend) and anti-human CD14 (clone M5E2; BioLegend) antibodies were injected i.v. into RICH mice (50 μg per mouse) 24 h before parasite infection. All studies involving mice were approved by the Institutional Animal Care and Use Committee of NUS and MIT.

***P. falciparum* Culture and Infection.** *P. falciparum* strain 3D7 was obtained from Malaria Research and Reference Reagent Resource and maintained in leukocyte-free human erythrocytes in malaria culture medium (MCM) (10.43 g RPMI 1640 powder, 25 mL 1 M Hepes buffer, 2 g $NaHCO_3$, 5 g Albumax, 25 mg gentamicin in 1 L milli-Q water) as described by Trager and Jensen (28). The parasites were treated with trypsin/chymotrypsin for 1 h at 37 °C with shaking before purification of schizonts to prevent the reinvasion of residual RBCs (29). The late-stage schizonts were purified by Percoll gradient centrifugation according to the protocol of Fernandez et al. (30).

For in vivo infection, synchronized ring-stage 3D7 parasites were prepared by sorbitol synchronization. Briefly, 10–12 h postinvasion cultures were spun down at 600 × *g* for 5 min and were incubated in 5% (vol/vol) sorbitol for 10 min at room temperature. Cells were washed three times in MCM medium. When parasitemia reached ∼10%, the blood was harvested, treated with trypsin/chymotrypsin, and then injected i.v. into humanized mice. Every RICH mouse was injected with 5×10^6 ring-stage parasites.

To set up in vitro NK cells, RBCs, and parasite coculture, human NK cells were purified from PBMCs using the EasySep Human CD56 Positive Selection Kit (Stem Cell Technologies). Human NK cells (with a purity of >95%) were mixed with purified late-stage schizonts at a ratio of 10:1, and then additional human RBCs were added to make a starting parasitemia of 0.2% (NK:schizonts:RBC = 10:1:250). For transwell experiments, RBCs and parasites were seeded in the bottom wells of a 24-well plate (Millipore), and NK cells were seeded in the transwell at the same ratio. Cells were cultured at 37 °C, and samples were taken at various time points for flow cytometry analysis of NK cell activation and parasite infection of RBCs. Blocking antibodies against human NKp30 (P30-15), NKp44 (P44-8), NKp46 (9E2), NKG2D (1D11), CD2 (RPA-2.10), 2B4 (C1.7), DNAM-1 (11A8), CD11a (HI111), and CD18 (TS1/18) were purchased from BioLegend and used at a concentration of 1 μg/mL CM A was purchased from Sigma and used in culture at a final concentration of 1 nM.

Antibodies, Flow Cytometry, and ELISA. The following antibodies were used for flow cytometry: anti-human CD45 (2D1) from BD Biosciences and anti-human CD14 (HCD14), CD56 (MEM-188), CD19 (HIB19), CD3 (HIT3a), CD235ab (HIR2), CD69 (FN50), and anti-mouse CD45.1 (A20) from BioLegend. Cell suspensions of PBMCs and RBCs were stained with appropriate antibodies in 100 μL PBS containing 0.2% BSA and 0.05% sodium azide for 30 min on ice. Stained cells were analyzed by flow cytometry using LSR II, and data were analyzed by FACS Diva (BD Biosciences) or FlowJo (TreeStar Inc.). To measure human cytokines by ELISA, blood from humanized mice was centrifuged at 1,500 × *g* for 5 min at 4 °C. Serum was used to quantify human cytokines IFN-γ and IL-6 using ELISA kits (BioLegend) following the manufacturer's protocol.

Imaging. NK cells (1×10^4) were incubated with 1×10^4 3D7 parasite-infected RBCs (10% parasitemia, synchronized) in MCM medium on a culture slide made by mounting a polydimethylsiloxane chamber on a Menzel-Gläser 22 × 60 mm #1 glass coverslip. The culture slide was placed in a Tokai Hit INU Live Cell Microscope Chamber in which the temperature was maintained at 37 °C in an atmosphere of 5% CO_2 and 3% O_2. Live-cell images were acquired on an inverted Olympus IX71 fitted with an Olympus Planapo 60×/1.4 oil lens using a Hamamatsu ORCA-ER (C4742-80–12AG) CCD camera.

Statistical Analysis. Data are presented as mean ± SEM. Differences between groups were analyzed via Student *t* test. A *P* value <0.05 was considered statistically significant. All calculations were performed using the Origin 8.0 software package.

ACKNOWLEDGMENTS. We thank Farzad Olfat for administrative support. This work was supported by the National Research Foundation Singapore through the Singapore–MIT Alliance for Research and Technology's Interdisciplinary Research Group in Infectious Disease Research Program.

1. Moreno A, Pérignon JL, Morosan S, Mazier D, Benito A (2007) Plasmodium falciparum-infected mice: More than a tour de force. *Trends Parasitol* 23(6):254–259.
2. Badell E, et al. (2000) Human malaria in immunocompromised mice: An in vivo model to study defense mechanisms against Plasmodium falciparum. *J Exp Med* 192(11):1653–1660.
3. Moore JM, Kumar N, Shultz LD, Rajan TV (1995) Maintenance of the human malarial parasite, Plasmodium falciparum, in scid mice and transmission of gametocytes to mosquitoes. *J Exp Med* 181(6):2265–2270.
4. Tsuji M, Ishihara C, Arai S, Hiratai R, Azuma I (1995) Establishment of a SCID mouse model having circulating human red blood cells and a possible growth of Plasmodium falciparum in the mouse. *Vaccine* 13(15):1389–1392.
5. Jiménez-Díaz MB, et al. (2009) Improved murine model of malaria using Plasmodium falciparum competent strains and non-myelodepleted NOD-scid IL2Rgammanull mice engrafted with human erythrocytes. *Antimicrob Agents Chemother* 53(10):4533–4536.
6. Vaughan AM, et al. (2012) Complete Plasmodium falciparum liver-stage development in liver-chimeric mice. *J Clin Invest* 122(10):3618–3628.
7. Stevenson MM, Riley EM (2004) Innate immunity to malaria. *Nat Rev Immunol* 4(3):169–180.
8. Millington OR, Di Lorenzo C, Phillips RS, Garside P, Brewer JM (2006) Suppression of adaptive immunity to heterologous antigens during Plasmodium infection through hemozoin-induced failure of dendritic cell function. *J Biol* 5(2):5.
9. Mannoor MK, et al. (2001) Resistance to malarial infection is achieved by the cooperation of NK1.1(+) and NK1.1(-) subsets of intermediate TCR cells which are constituents of innate immunity. *Cell Immunol* 211(2):96–104.
10. Ariyasinghe A, et al. (2006) Protection against malaria due to innate immunity enhanced by low-protein diet. *J Parasitol* 92(3):531–538.
11. Kitaguchi T, Nagoya M, Amano T, Suzuki M, Minami M (1996) Analysis of roles of natural killer cells in defense against Plasmodium chabaudi in mice. *Parasitol Res* 82(4):352–357.
12. Artavanis-Tsakonas K, et al. (2003) Activation of a subset of human NK cells upon contact with Plasmodium falciparum-infected erythrocytes. *J Immunol* 171(10):5396–5405.
13. Artavanis-Tsakonas K, Riley EM (2002) Innate immune response to malaria: Rapid induction of IFN-gamma from human NK cells by live Plasmodium falciparum-infected erythrocytes. *J Immunol* 169(6):2956–2963.
14. Korbel DS, Newman KC, Almeida CR, Davis DM, Riley EM (2005) Heterogeneous human NK cell responses to Plasmodium falciparum-infected erythrocytes. *J Immunol* 175(11):7466–7473.
15. Cerwenka A, Lanier LL (2001) Natural killer cells, viruses and cancer. *Nat Rev Immunol* 1(1):41–49.
16. Chen Q, Khoury M, Chen J (2009) Expression of human cytokines dramatically improves reconstitution of specific human-blood lineage cells in humanized mice. *Proc Natl Acad Sci USA* 106(51):21783–21788.
17. Lanier LL (2005) NK cell recognition. *Annu Rev Immunol* 23:225–274.
18. Tangpukdee N, Krudsood S, Kano S, Wilairatana P (2012) Falciparum malaria parasitemia index for predicting severe malaria. *Int J Lab Hematol* 34(3):320–327.
19. de Villartay JP, Rouger P, Muller JY, Salmon C (1985) HLA antigens on peripheral red blood cells: Analysis by flow cytofluorometry using monoclonal antibodies. *Tissue Antigens* 26(1):12–19.
20. Agudelo O, Bueno J, Villa A, Maestre A (2012) High IFN-gamma and TNF production by peripheral NK cells of Colombian patients with different clinical presentation of Plasmodium falciparum. *Malar J* 11:38.
21. Newman KC, Korbel DS, Hafalla JC, Riley EM (2006) Cross-talk with myeloid accessory cells regulates human natural killer cell interferon-gamma responses to malaria. *PLoS Pathog* 2(12):e118.
22. Roetynck S, et al. (2006) Natural killer cells and malaria. *Immunol Rev* 214:251–263.
23. Shibuya K, et al. (1999) Physical and functional association of LFA-1 with DNAM-1 adhesion molecule. *Immunity* 11(5):615–623.
24. Barber DF, Faure M, Long EO (2004) LFA-1 contributes an early signal for NK cell cytotoxicity. *J Immunol* 173(6):3653–3659.
25. Ihanus E, Uotila LM, Toivanen A, Varis M, Gahmberg CG (2007) Red-cell ICAM-4 is a ligand for the monocyte/macrophage integrin CD11c/CD18: Characterization of the binding sites on ICAM-4. *Blood* 109(2):802–810.
26. Washburn ML, et al. (2011) A humanized mouse model to study hepatitis C virus infection, immune response, and liver disease. *Gastroenterology* 140(4):1334–1344.
27. Chen Q, et al. (2013) Human fetal hepatic progenitor cells are distinct from, but closely related to, hematopoietic stem/progenitor cells. *Stem Cells* 31(6):1160–1169.
28. Trager W, Jensen JB (1976) Human malaria parasites in continuous culture. *Science* 193(4254):673–675.
29. Thompson JK, Triglia T, Reed MB, Cowman AF (2001) A novel ligand from Plasmodium falciparum that binds to a sialic acid-containing receptor on the surface of human erythrocytes. *Mol Microbiol* 41(1):47–58.
30. Fernandez V, Treutiger CJ, Nash GB, Wahlgren M (1998) Multiple adhesive phenotypes linked to rosetting binding of erythrocytes in Plasmodium falciparum malaria. *Infect Immun* 66(6):2969–2975.

Supporting Information

Chen et al. 10.1073/pnas.1323318111

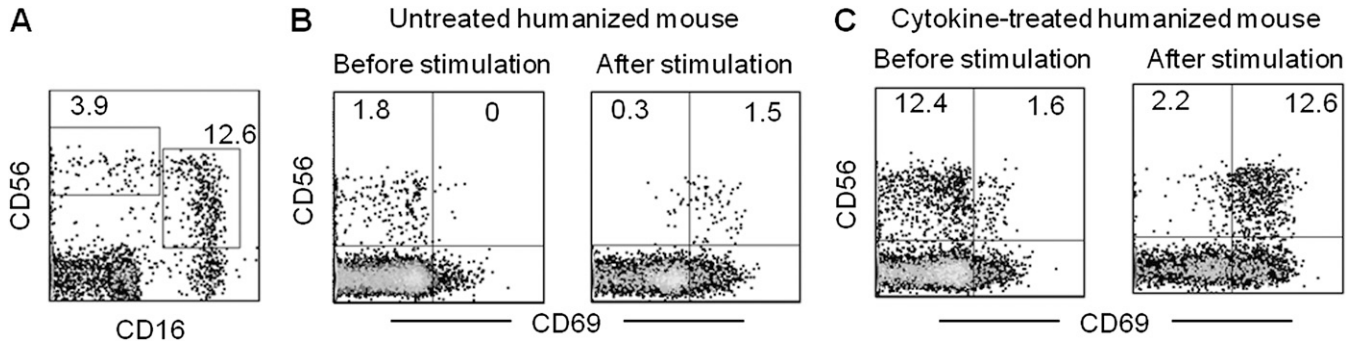

Fig. S1. Phenotype and activation status of human natural killer (NK) cells in cytokine-treated humanized mice. (*A*) Seven days after cytokine plasmid injection, peripheral blood mononuclear cells (PBMCs) from the treated humanized mice were stained for mouse CD45, human CD45, and CD56 plus CD16. Shown is the CD16 vs. CD56 staining profile gating on human $CD45^+$ cells. (*B* and *C*) PBMCs from cytokine-treated and nontreated humanized mice were stimulated ex vivo with 1 μg/mL human IL-15 for 10 h. Cells were stained as above. Shown are the staining profiles of CD56 vs. CD69 (gating on human $CD45^+$ cells) before and after stimulation.

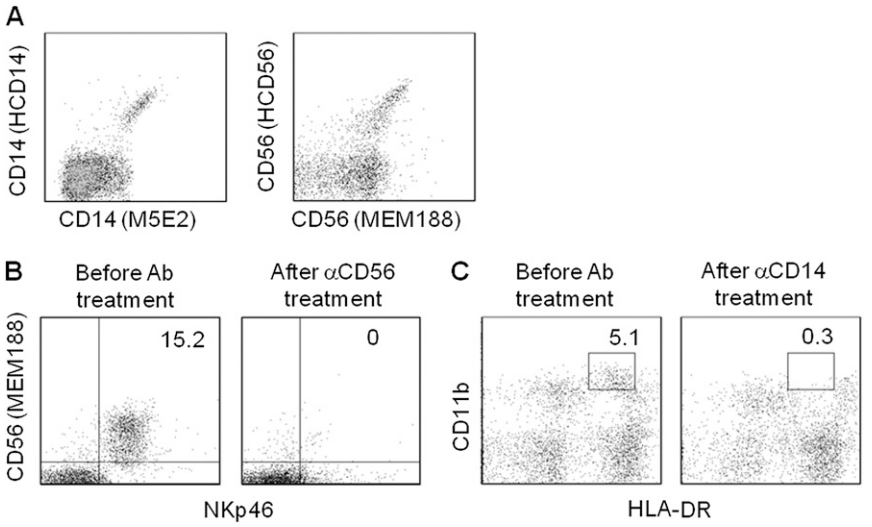

Fig. S2. Antibody-mediated depletion of human NK cells and monocytes/macrophages in RBC-supplemented, immune cell-optimized humanized (RICH) mice. (*A*) Evaluation of antibody staining of NK cells and monocytes/macrophages. Seven days after cytokine plasmid injection, PBMCs were stained with FITC-hCD45, PE-Cy7-mCD45, plus PE-CD14 (HCD14) and APC-CD14 (M5E2) or PE-CD56 (HCD56) and APC-CD56 (MEM188) antibodies. Shown are CD14 (M5E2) vs. CD14 (HCD14) and CD56 (MEM188) vs. CD56 (HCD56) staining profiles gating on human $CD45^+$ cells. (*B* and *C*) Depletion of NK cells and monocytes/macrophages. PBMCs were obtained from mice treated with IL-15 and Flt-3/Flk-2 ligand before and 24 h after injection with anti-CD56 (HCD56) or anti-CD14 (M5E2) antibodies. Cells were stained for mCD45, hCD45, plus CD56 (MM188) and NKp46 or CD11b and HLA-DR. Shown are NKp46 vs. CD56 (MEM188) and HLA-DR vs. CD11b staining profiles gating on human $CD45^+$ cells. The numbers indicate percentages of cells in the gated areas.

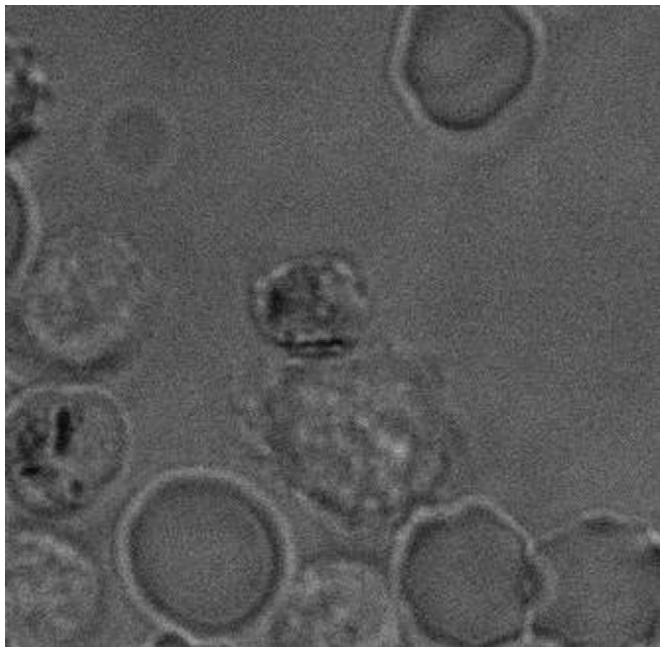

Fig. S3. Migration and adhesion of human NK cells to parasite-infected RBCs. Purified human NK cells were mixed with asynchronized *Plasmodium falciparum*-infected RBCs (10% parasitemia) at a ratio of 10:1 and placed in a temperature-, O_2-, and CO_2-controlled chamber on an inverted microscope. The video was started 2 h after incubation.

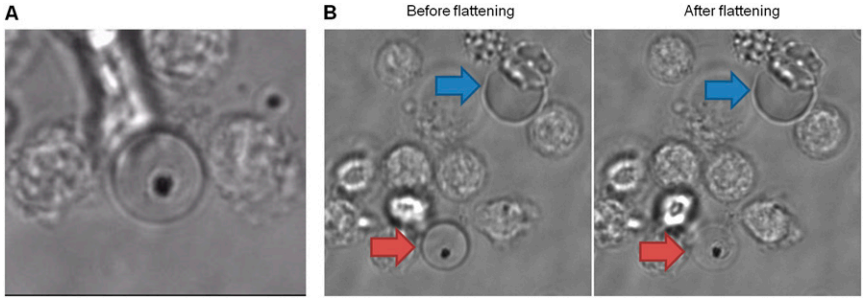

Fig. S4. The flattening of iRBCs after contact with NK cells. Purified human NK cells were mixed with asynchronized *P. falciparum*-infected RBCs (10% parasitemia) at a ratio of 10:1 and were placed in a temperature-, O_2-, and CO_2-controlled chamber on an inverted microscope. (*A*) The video was started 8 h after incubation. (*B*) Images taken from video before and after iRBC flattening. The red arrows indicate the infected RBCs. The blue arrows indicate normal RBCs.